Cell Reports, Volume ■ ■

Supplemental information

Tolerance to extracellular acidic pH facilitates tumor plasticity

Manami Hasegawa, Bo Xu, Keisuke Maeda, Motoaki Seki, FeiFei Cai, Runmei Cui, Ritsuko Ando, Suzuka Nakagawa, Ayana Sakamoto, Cayla Boycott, Hiroyuki Yatabe, Miyuki Nishida, Ken Matsumoto, Chisato Iwabuchi-Yoshida, Sho Aki, Kazuyuki Yamagata, Rika Tsuchida, Mami Takahashi, Futoshi Kuribayashi, Hiroyasu Kidoya, Hiroshi Hirata, Shingo Matsumoto, Shinsuke Sando, Hideyuki Yanai, Nozomu Yachie, and Tsuyoshi Osawa

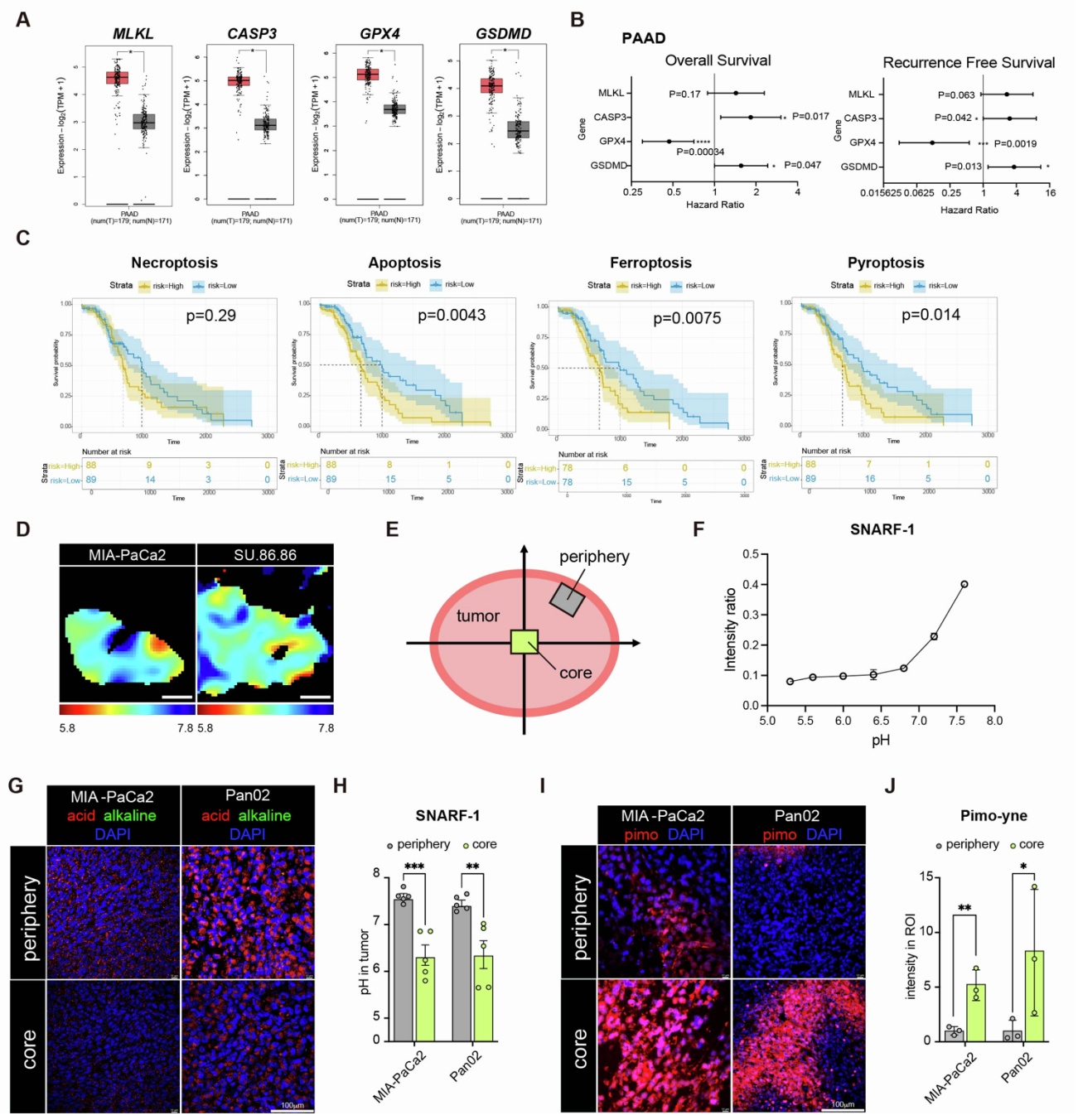

Figure S1. Cell death–related gene signatures predict prognosis, and acidic tumor regions are observed *in vivo* (related to Figure 1).

(**A**) *MLKL/CASP3/GPX4/GSDMD* expression levels in pancreatic ductal adenocarcinoma (PAAD) tissues (left) and normal tissues (right) from PAAD patients in the TCGA database, analyzed using the GEPIA2 online platform.

(**B**) Forest plots showing the hazard ratios (HRs) and 95% confidence intervals (CIs) of four representative genes (*MLKL/CASP3/GPX4/GSDMD*) for overall survival (OS, left) and relapse-free survival (RFS, right) in patients with pancreatic adenocarcinoma from the TCGA database. The HRs were calculated using

univariate Cox regression analysis. P values are indicated next to each gene; asterisks denote levels of statistical significance. *$p < 0.05$.

(**C**) Kaplan–Meier survival curves of high-risk and low-risk PAAD patients from the GEO database, categorized based on necroptotic genes (*RIPK1, RIPK3, MLKL, FADD, TNFR1, TRADD*), apoptotic genes (*BAX, BAK, CYCS, CASP9, CADP3, TP53*), ferroptotic genes (G*PX4, SLC7A11, ACSL4, ALOX15, TFRC, FTH1*), and pyroptotic genes (*CADP1, GSDMD, NLRP3, IL-1B, CASP4, ASC*) expression.

(**D**) Extracellular pH maps of MIA-PaCa2 and SU.86.68 xenograft tumors measured by EPR imaging. The white scale bar represents 5 mm.

(**E**) Schematic illustrating the definition of core and periphery regions in Pan02 or MIA-PaCa2 tumors at an approximate volume of 1,000 mm^3.

(**F**) SNARF-1 calibration curve (n = 3). Intensity ratios were calculated as OD_{480}/OD_{640}.

(**G**) Representative images of syngeneic Pan02 tumors showing acidic (red) and alkaline (green) signals detected by the ratiometric pH-sensitive fluorescent dye SNARF-1 following intravenous injection. The tumor core and periphery regions are shown and compared.

(**H**) Quantification of tumor pH in the images shown in (**G**) using the SNARF-1 calibration curve shown in (F). Data are represented as means ± SEM n = 3 biological replicates. Statistical analysis was performed by one-way ANOVA. **$P < 0.01$; ***$P < 0.005$.

(**I**) Representative images of syngeneic Pan02 tumors and MIA-PaCa2 xenograft tumors stained for pimonyne (red), a chemical indicator of tumor hypoxia. Hypoxic signals in the tumor core and periphery regions are shown and compared.

(**J**) Quantification of tumor hypoxia in the images shown in (I). Data are represented as means ± SEM n = 3 biological replicates. Statistical analysis was performed by one-way ANOVA. *$P < 0.05$; **$P < 0.01$.

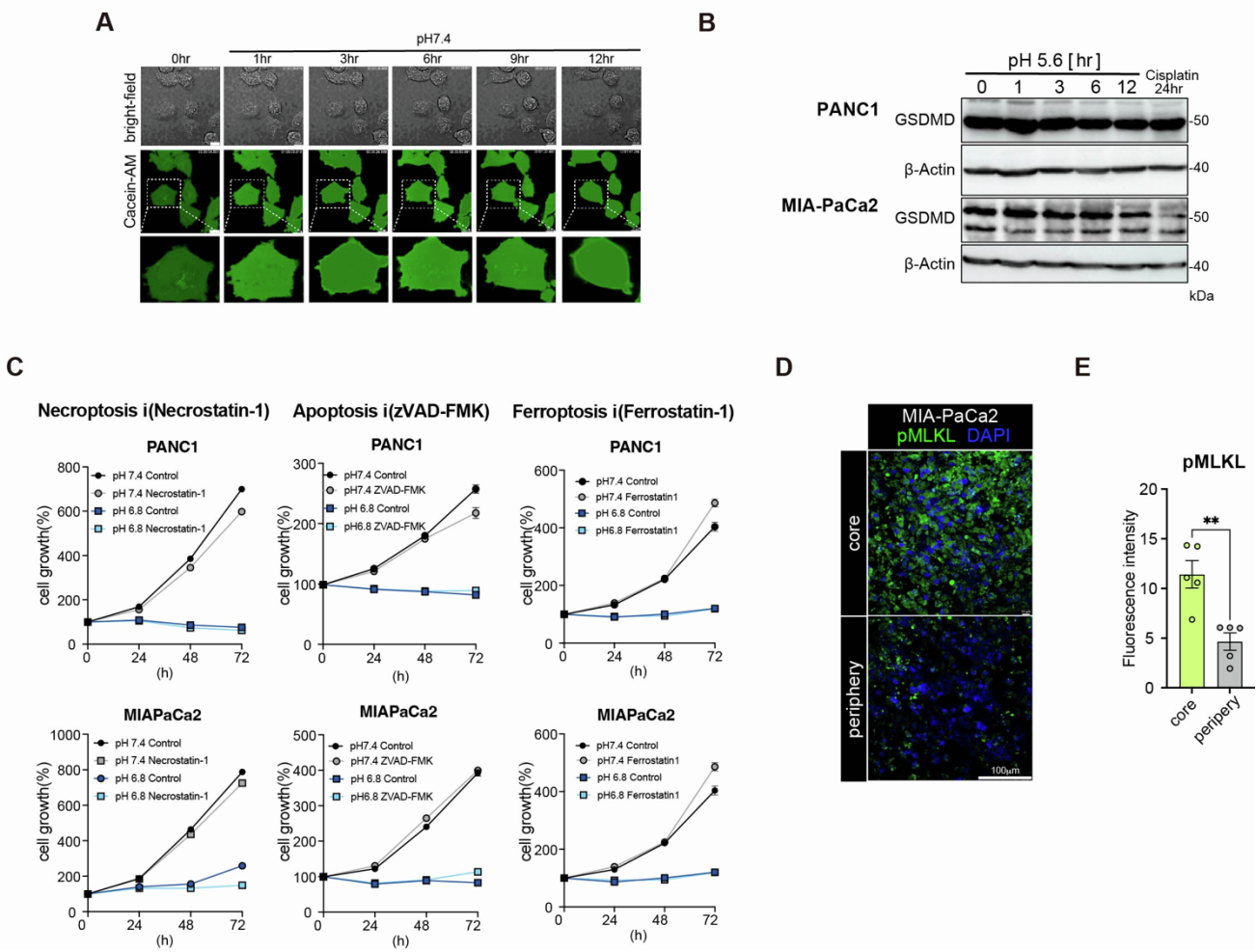

Figure S2. Expanded quantification of acidic pH–induced cell death (related to Figure 1).

(**A**) Time-lapse imaging of Calcein AM-stained MIA-PaCa2 cells showing no significant release of cellular contents under pH 7.4 conditions. Scale bars, 10 μm.

(**B**) Western blot analysis of GSDMD protein levels in PANC1 and MIA-PaCa2 cells exposed to pH 5.6 from 0 h to 12 h.

(**C**) Time-course analysis of cell proliferation in PANC1 and MIA-PaCa2 cells cultured under pH 7.4 or pH 6.8 in the presence of a necroptosis inhibitor (Necrostatin-1, left), apoptosis inhibitor (Z-VAD-FMK, center), or ferroptosis inhibitor (Ferrostatin-1, right). Proliferation was assessed at 24-, 48-, and 72-hours using SRB assays. Data are represented as means ± SEM n = 3 biological replicates.

(**D**) Immunofluorescence staining of MIA-PaCa2 xenograft tumors collected from mice described in panel (tumor core and periphery). The indicated marker pMLKL (a marker of necroptosis) is shown. Nuclei were counterstained with DAPI. Scale bars, 100 μm.

(**E**) Quantification of pMLKL$^+$ signal intensity within the ROI shown a in (**D**). Data are represented as means ± SEM n = 5 biological replicates. Statistical analysis was performed by one-way ANOVA. $^{**}P < 0.01$.

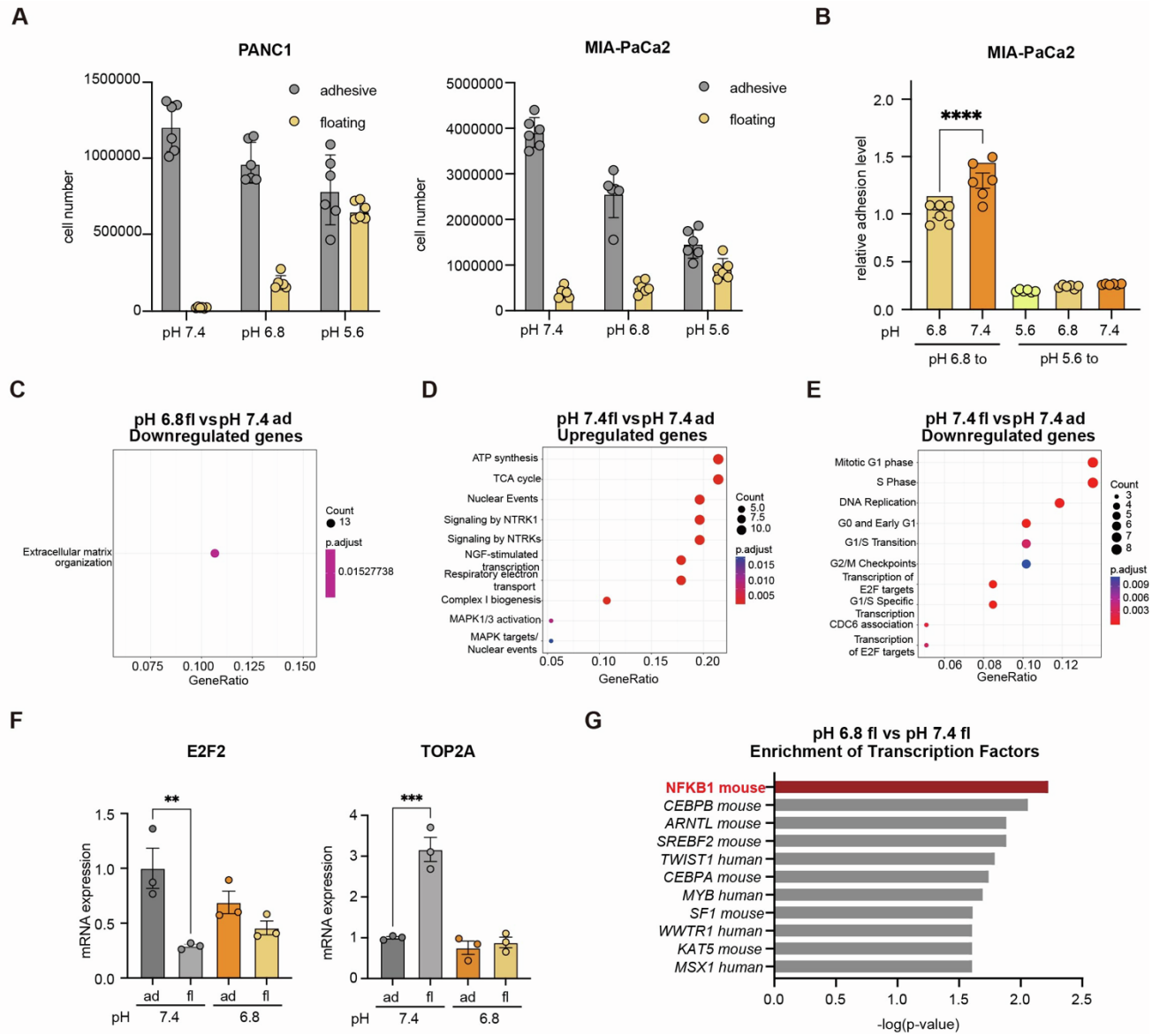

Figure S3. Additional analyses of pathways activated in floating cells at pH 6.8 (related to Figure 2).

(**A**) Total cell numbers under each pH condition from the experiment shown in Figure 2A, in which the proportions of floating and adherent cells were calculated for PANC1 and MIA-PaCa2 cells. Data are represented as means ± SEM n = 6 biological replicates.

(**B**) Quantification of adhesion recovery in MIA-PaCa2 cells based on proliferation assays described in Figure 2A. Data are represented as means ± SEM n = 6 biological replicates. Statistical analysis was performed by one-way ANOVA. ****$P < 0.001$.

(**C** to **E**) Gene ontology (GO) enrichment analysis of molecular function terms for downregulated differentially expressed genes (DEGs) between pH 6.8 floating and pH 6.8 adhesive cells (**C**), upregulated DEGs between pH 7.4 floating and pH 7.4 adhesive cells (**D**), and downregulated DEGs between pH 7.4

floating and pH 7.4 adhesive cells (**E**). Dot plots display GO terms enriched among DEGs, and Dot color represents the p-value, and dot size indicates the count of DEGs associated with each GO term.
(**F**) mRNA expression level of *E2F2* (mitotic regulator gene) and *TOP2A* (type II topoisomerase gene) in PANC1 adherent and floating cells under pH 7.4 and pH 6.8. Data are represented as means ± SEM n = 3 biological replicates. Statistical analysis was performed by one-way ANOVA. $^{**}P < 0.01$; $^{***}P < 0.005$.
(**G**) Transcription factor (TF) enrichment analysis of genes upregulated in pH 7.4 floating compared to pH 6.8 floating cells. P-values were adjusted for multiple comparisons using the Benjamini–Hochberg method.

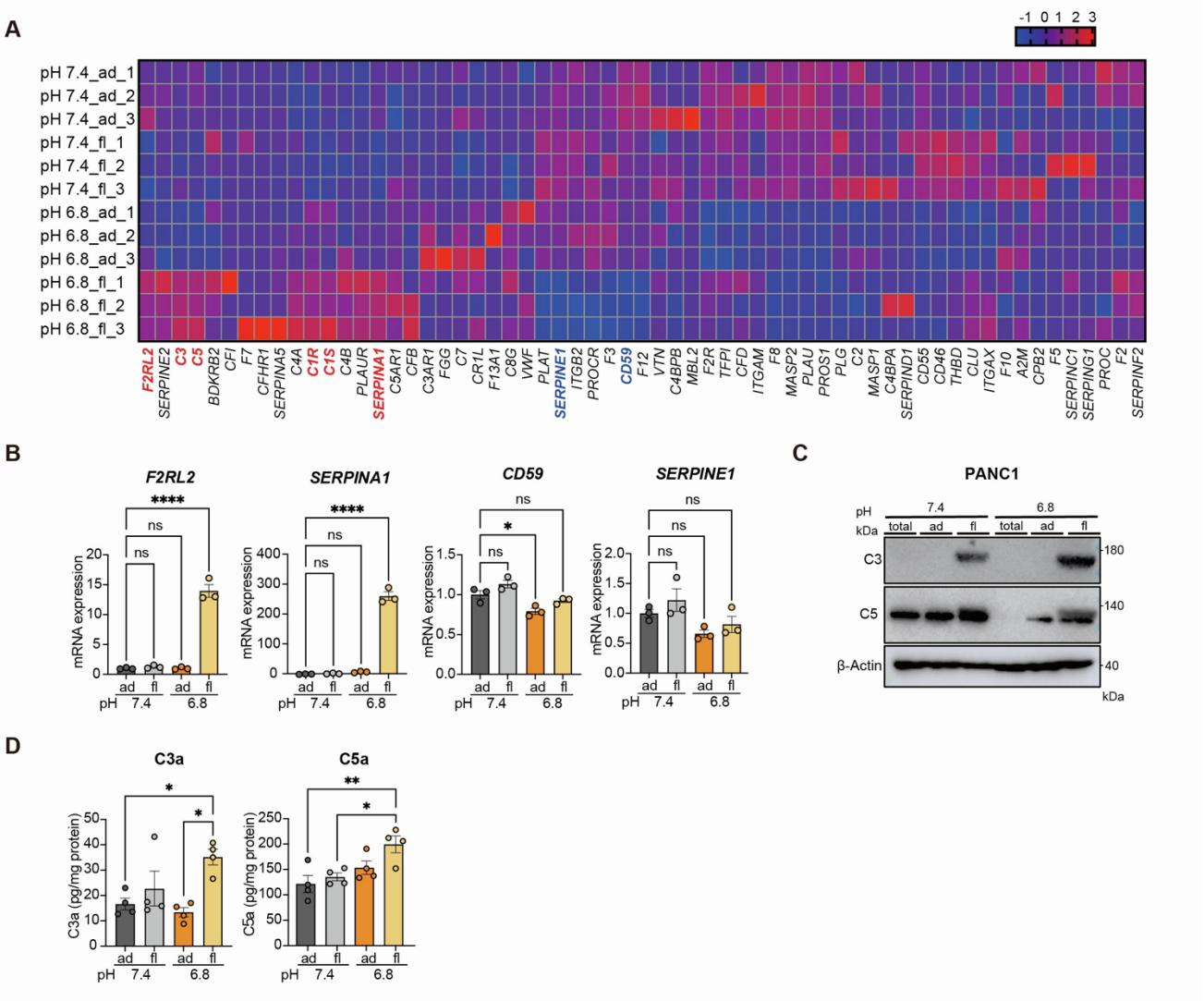

Figure S4. Activation of the complement pathway in floating cells at pH 6.8 (related to Figure 2).

(**A**) Heatmap of genes enriched in the complement and coagulation cascades in floating and adherent cells cultured at pH 6.8 or pH 7.4. Genes shown in red are upregulated, whereas genes shown in blue are downregulated in floating cells at pH 6.8 relative to pH 7.4.

（**B**）mRNA expression levels of the genes labeled in (**A**) in adherent and floating PANC1 cells under pH 7.4 and pH 6.8. Data are represented as means ± SEM n = 3 biological replicates. Statistical analysis was performed by one-way ANOVA. **P* < 0.05; *****P* < 0.001; ns: not significant.

(**C**) Western blot analysis of complement activation markers, C3 and C5, in PANC1 cells. Cells were cultured at pH 6.8 for 24 h, after which adherent (ad) and floating (fl) cell populations were separated and analyzed.

(**D**) ELISA analysis of complement activation markers, C3a and C5a, in PANC1 cells. Cell lysates were collected and analyzed; culture supernatants were not used. Data are represented as means ± SEM n = 4 biological replicates. Statistical analysis was performed by one-way ANOVA. **P* < 0.05; ***P* < 0.01.

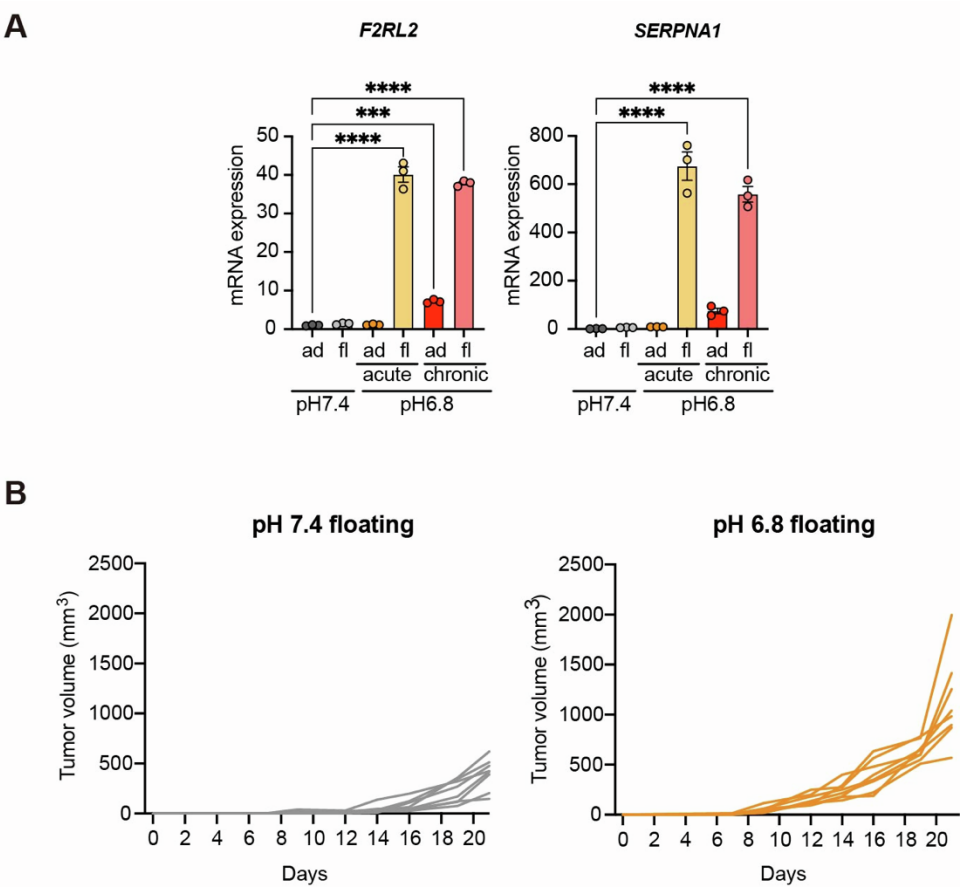

Figure S5. Floating cells under pH 6.8 retain tumorigenic potential (related to Figure 3).

(**A**) mRNA expression levels of the complement pathway (*F2RL2, SERPNA1*) in adherent and floating PANC1 cells cultured under pH 7.4 and pH 6.8 during acute and chronic exposure. Data are represented as means ± SEM n = 3 biological replicates. Statistical analysis was performed by one-way ANOVA. ****P* < 0.005; *****P* < 0.001.

(**B**) Tumor growth curves of individual mice in Figure 2C. Floating MIA-PaCa2 cells cultured under pH 7.4 or pH 6.8 were isolated from each condition and injected subcutaneously into mice at a dose of 5 × 10^6 cells. (n = 8 per group).

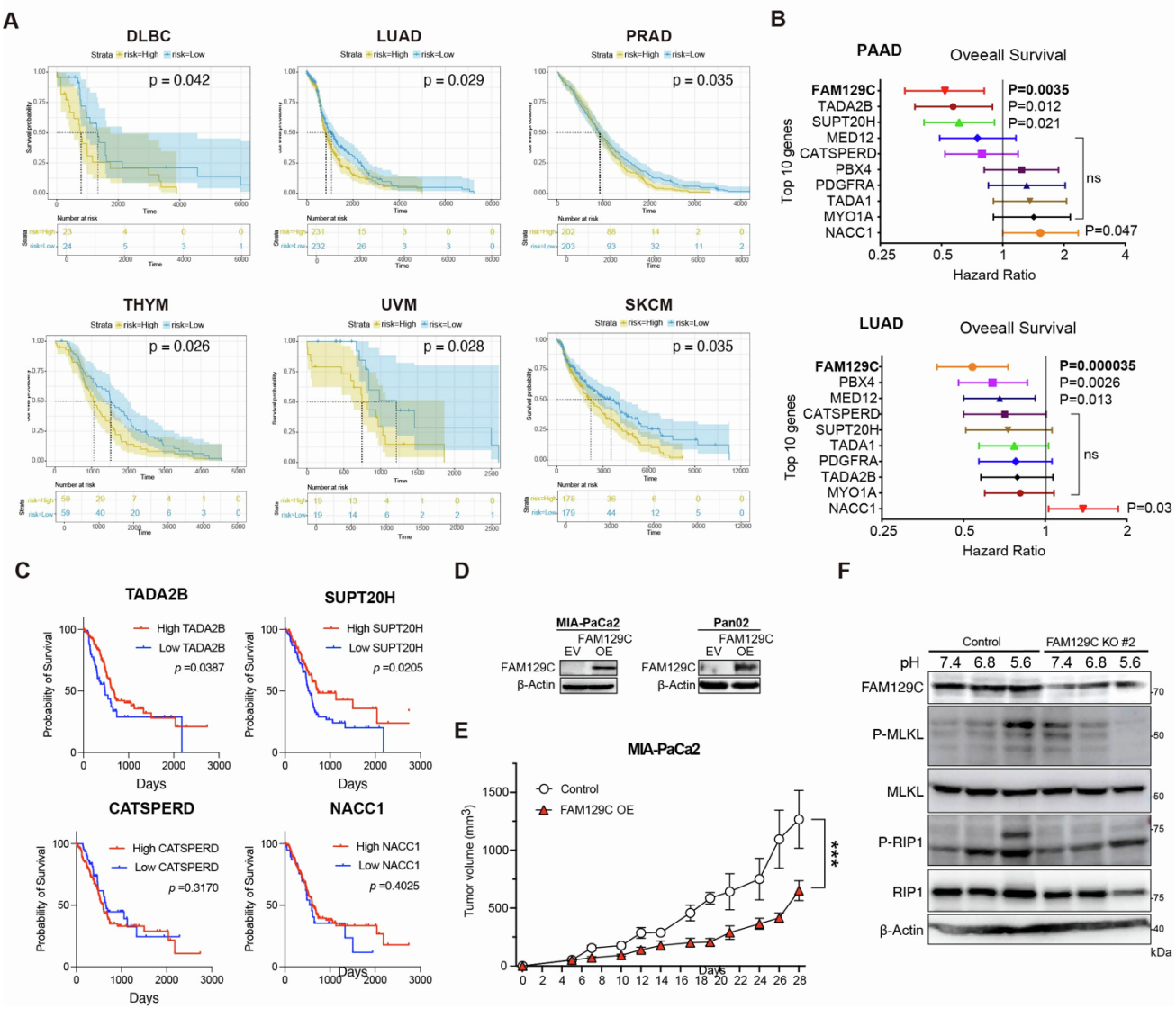

Figure S6. Acid tolerance–related genes show a positive association with malignancy across multiple cancer types (related to Figure 4).

(**A**) Overall survival of patients with lymphoid neoplasm diffuse large B-cell lymphoma (DLBC), lung adenocarcinoma (LUAD), prostate adenocarcinoma (PRAD), thymoma (THYM), uveal melanoma (UVM), and skin cutaneous melanoma (SKCM). Patients were stratified into high-risk (log risk > 0) and low-risk (log risk < 0) groups based on the Cox proportional hazards model, using the expression levels of the top 10 upregulated genes under acidic pH conditions identified in CRISPR knockout screening (*MED12*, *TADA1*, *PBX4*, *MYO1A, PDGFRA*, *FAM129C*, *TADA2B*, *SUPT20H*, *CATSPERD*, *NACC1*) (Figure 3B).

(**B**) Prognostic impact of top 10 CRISPR-identified genes in PAAD and LUAD. Forest plots showing hazard ratios (HRs) and 95% confidence intervals for the top 10 genes associated with overall survival in pancreatic (PAAD, left) and lung adenocarcinoma (LUAD, right). HRs were calculated from expression data; *p*-values are shown for significant genes. ns: not significant.

(**C**) Prognostic analysis of gRNA-targeted genes ranked 7th to 10th in pancreatic cancer. Genes ranked 1st to 6th are shown in Figure 4D.

(**D**) Western blot analysis confirming the establishment of FAM129C-overexpressing MIA-PaCa2 and Pan02 cells.

(**E**) Tumor growth curves of control and FAM129C-overexpressing MIA-PaCa2 xenografts. Cells were injected subcutaneously into SCID mice at a dose of 5×10^6 cells. Data are represented as means ± SEM (n = 5 biological replicates). Statistical analysis was performed by the unpaired two-tailed Student's t-test. ***$P < 0.005$.

(**F**) Western blot analysis of key necroptosis markers in control and FAM129C knockout PANC1 cells cultured under different pH conditions. Cells were incubated for 24 hours at pH 7.4 or pH 6.8 and for 6 hours at pH 5.6.

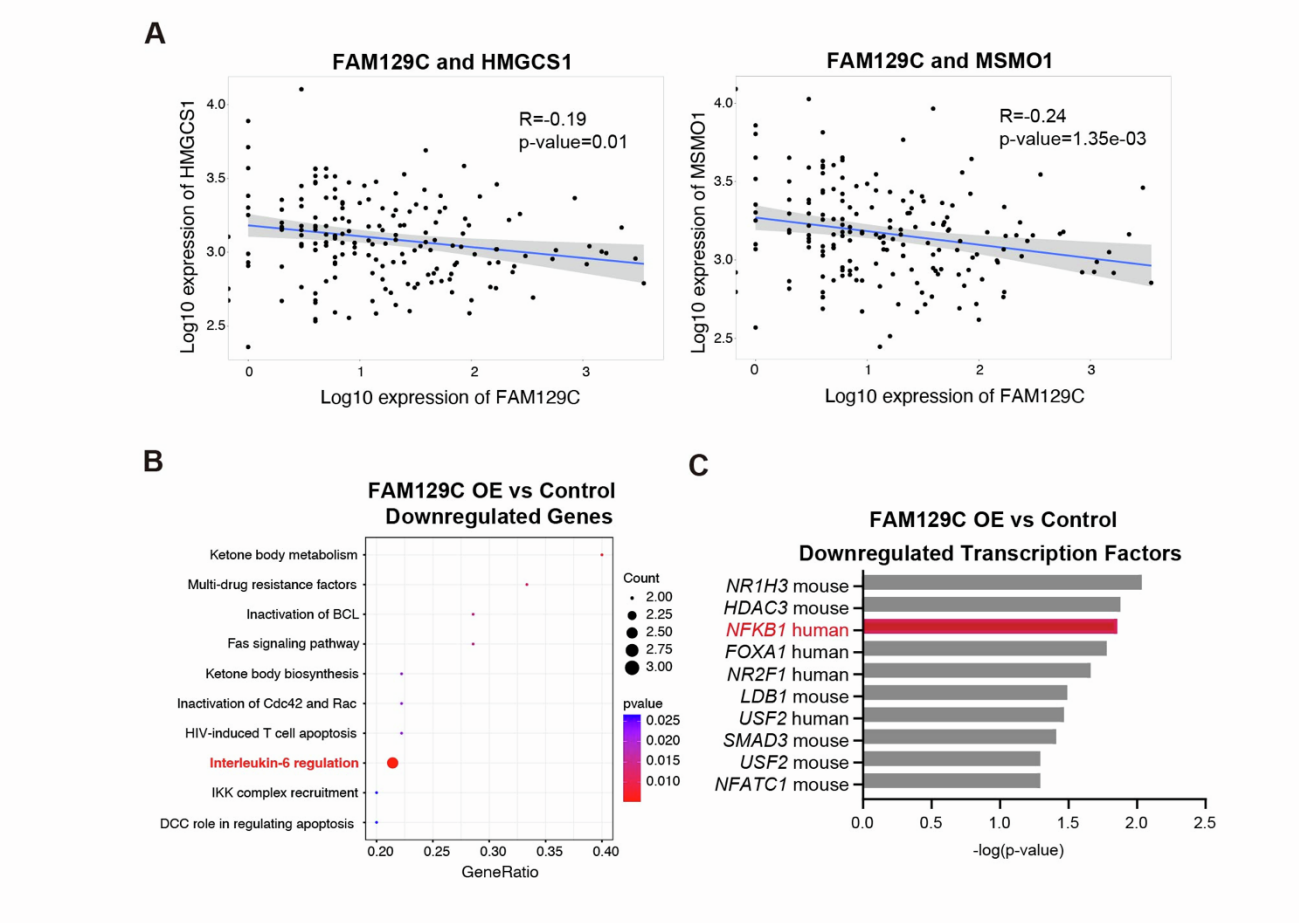

Figure S7. Potential links between FAM129C and downstream signaling under acidic conditions (related to Figure 5).

(**A**) Correlation of *FAM129C* expression with *HMGCS1* (left) and *MSMO1* (right) in the TCGA pancreatic ductal adenocarcinoma (PAAD) dataset. *HMGCS1* and *MSMO1* are key enzymes in the cholesterol biosynthesis pathway and were upregulated under acidic conditions (pH 6.8).

(**B**) Gene ontology analysis of molecular function terms for genes downregulated in FAM129C overexpression cells, compared with control cells. Dot plots display GO terms enriched among DEGs. Dot color represents the p-value, and dot size indicates the count of DEGs.

(**C**) Transcription factor (TF) enrichment analysis of genes downregulated in FAM129C overexpression compared to control cells. P-values were adjusted for multiple comparisons using the Benjamini–Hochberg method.

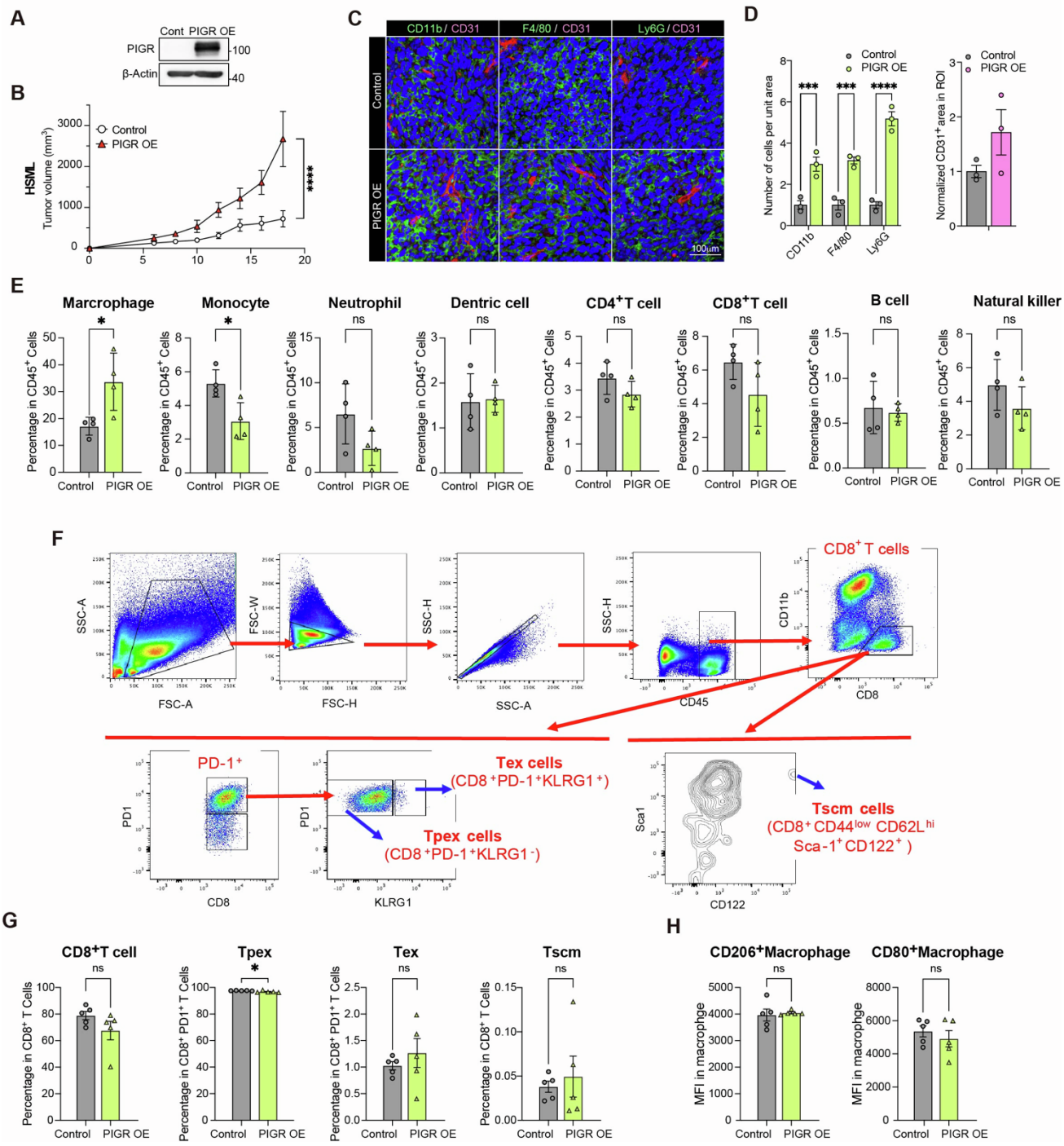

Figure S8. Expanded quantification of immune cell infiltration induced by PIGR overexpression (related to Figure 5).

(**A**) Western blot analysis confirming the establishment of PIGR-overexpressing HSML cells.

(**B**) Tumor growth curves of control and PIGR-overexpressing syngeneic HSML tumors. Cells were injected subcutaneously into C57BL/6J mice at a dose of 5 × 10^6 cells in. Data are represented as means ± SEM (n = 5 biological replicates). Statistical analysis was performed by the unpaired two-tailed Student's t-test. ****$P < 0.001$.

(**C**) Immunostaining of tumors excised from control and PIGR-overexpressing syngeneic HSML tumors. Vascular endothelial cells were labeled with CD31, myeloid cells with CD11b, macrophages with F4/80, and neutrophils with Ly6G. Nuclei were counterstained with DAPI. Scale bars, 100 μm.

(**D**) Quantification of numbers of $CD11b^+$, $F4/80^+$, and $Ly6G^+$ cells (left panel), and $CD31^+$ area (right panel) shown in (C). Data are represented as means ± SEM (n = 5 biological replicates). Statistical analysis was performed by the unpaired two-tailed Student's t-test. ***$P < 0.005$; ****$P < 0.001$.

(**E**) Proportions of $CD45^+$ immune cell subsets in control and PIGR-overexpressing syngeneic HSML tumors measured by flow cytometry (FACS). Data are represented as means ± SEM (n = 5 biological replicates). Statistical analysis was performed by the unpaired two-tailed Student's t-test. *$P < 0.05$; ns: not significant.

(**F**) Schematic of the experimental workflow and gating strategy for fluorescence-activated cell sorting (FACS) of $CD45^+$ immune cells isolated from syngeneic Pan02 tumors. $CD45^+$ cells were further gated to identify $CD8^+$ T cells ($CD45^+$ $F4/80^-$ $CD8^+$), exhaustion-associated $CD8^+$ T cells ($CD45^+$ $CD8^+$ $PD\text{-}1^+$) or stemness-associated $CD8^+$ T cells ($CD45^+$ $CD8^+$ CD44low CD62Lhigh $Sca\text{-}1^+$ $CD122^+$). Representative gating strategies are shown for control and PIGR-overexpressing syngeneic Pan02 tumors.

(G) Quantification of the proportions of $CD8^+$ T cell subsets in control and PIGR-overexpressing syngeneic Pan02 tumors. Cells were injected subcutaneously into C57BL/6J mice at a dose of 5×10^6 cells. Data are represented as means ± SEM (n = 5 biological replicates). Statistical analysis was performed by unpaired two-tailed Student's t-test. *$P < 0.05$; ns: not significant.

(H) Quantification of macrophage polarization in control and PIGR-overexpressing syngenic Pan02 tumors. M1-like macrophages were defined as $CD45^+$ $F4/80^+$ $CD11b^+$ $CD80^+$ cells, whereas M2-like macrophages were defined as $CD45^+$ $F4/80^+$ $CD11b^+$ $CD206^+$ cells. Data are represented as means ± SEM (n = 5 biological replicates). Statistical analysis was performed by the unpaired two-tailed Student's t-test. ns: not significant.

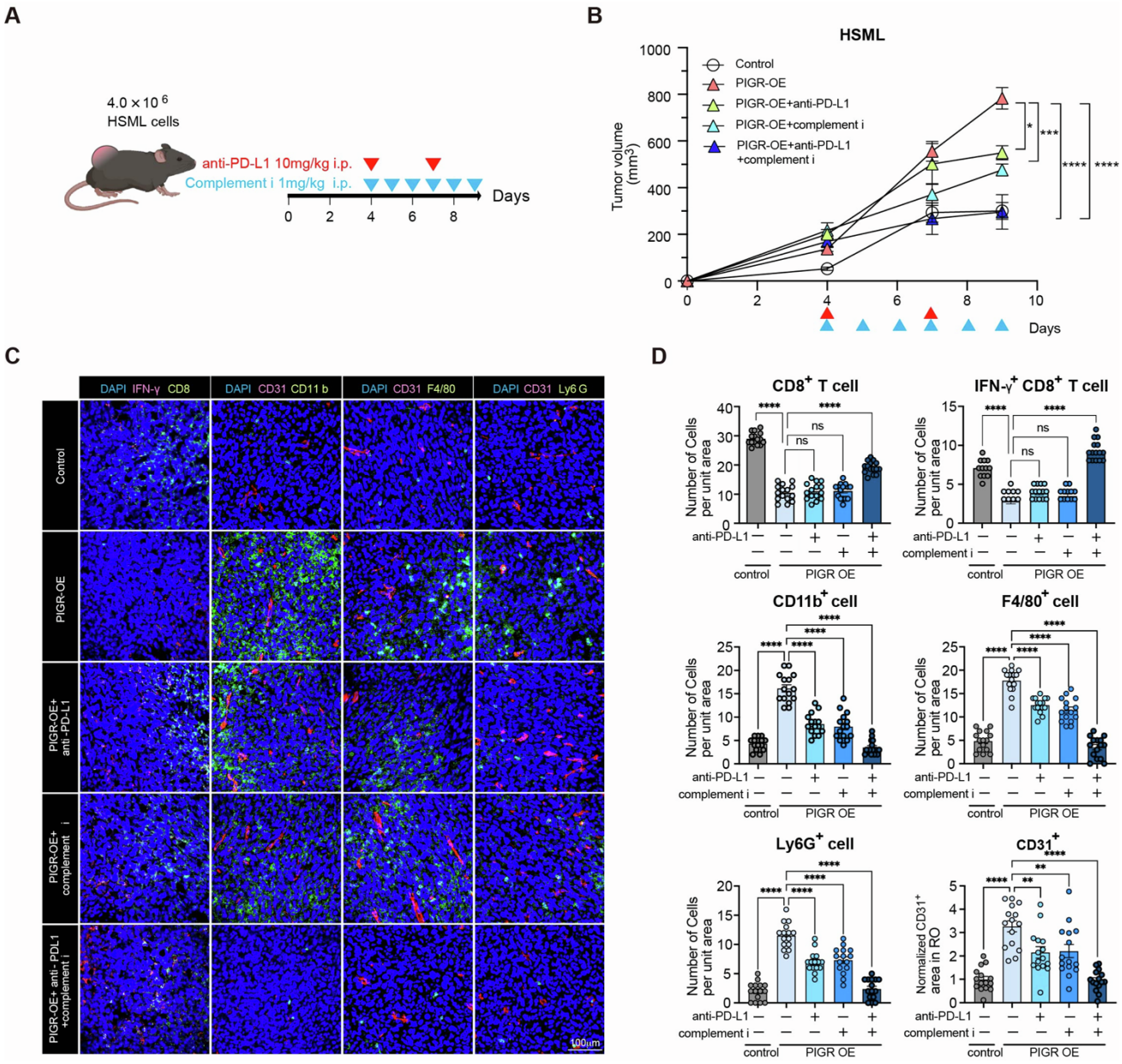

Figure S9. Anti–PD-L1 treatment and complement inhibition synergistically suppress PIGR-overexpressing HSML tumors (related to Figure 6).

(**A**) *In vivo* experiment scheme. Tumor cells (4×10^6 control or PIGR-overexpressing HSML cells) were subcutaneously injected into C57BL/6J mice. The control group received PBS from day 4, while PIGR-overexpressing groups were treated with either PBS from day 4, anti-PD-L1 antibody on days 4 and 7, PMX53 every day from day 4, or a combination of anti-PD-L1 antibody and PMX53 via i.p.

(**B**) Tumor growth curves of syngeneic Pan02 tumors described in (**A**). Tumor growth was monitored every 2 days (n = 5 mice per group). Tumor samples were collected for further analyses on day 10. Data are represented as means ± SEM of $n = 5$ biological replicates. Statistical analysis was performed by two-way ANOVA. *$P < 0.05$; ***$P < 0.005$; ****$P < 0.001$.

(**C**) Immunofluorescence staining of syngeneic Pan02 tumors collected from mice described in (A). The indicated markers are shown as follows: CD31 (vascular endothelial cells), CD11b (myeloid cells), F4/80 (macrophages), Ly6G (neutrophils), CD8 (cytotoxic T cells), and IFN-γ (IFN-γ–producing cells). Nuclei were counterstained with DAPI. Scale bars, 100 μm.

(**D**) Quantification of cell numbers of $CD8^+$ T cells, IFN-γ^+ $CD8^+$ T cells, CD11b, F4/80, and Ly6G and $CD31^+$ area in Figure 6C. Data are represented as means ± SEM of $n = 5$ biological replicates. Statistical analysis was performed by unpaired two-tailed Student's t-test. $^{**}P < 0.01$; $^{****}P < 0.001$; ns: not significant.

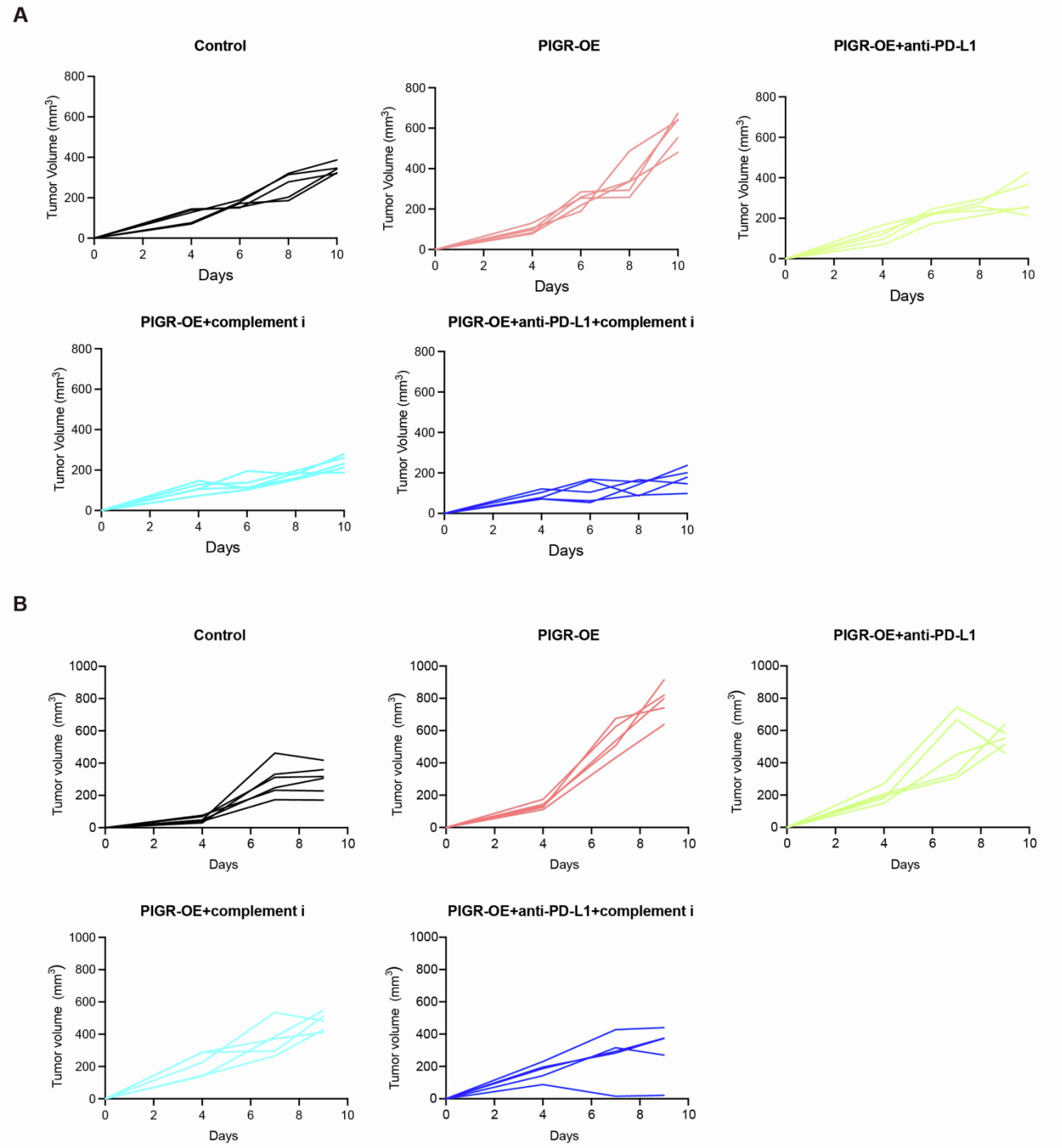

Figure S10. Tumor progression in individual Pan02- and HSML-bearing mice under different treatments (related to Figure 6).

(**A**) Tumor size progression in individual syngeneic Pan02 tumor–bearing mice from each treatment group shown in Figure 6B (n = 5 biological replicates).

(**b**) Tumor size progression in individual syngeneic HSML tumor–bearing mice from each treatment group shown in Figure S9B (n = 5 biological replicates).

Table S1. Primers for real-time PCR.

Primer	Forward Sequence	Reverse Sequence
h*ACTB*	5'-AGAAGGAGATCACTGCCCTGGCACC-3'	5'-CCTGCTTGCTGATCCACATCTGCTG-3'
h*HMGS1*	5'-CTCTTGGGATGGACGGTATGC-3'	5'-GCTCCAACTCCACCTGTAGG-3'
h*MSMO1*	5'-TATGCTGGTTCTCGGCATCAT-3'	5'-CCAAAAATTCGATCCCACCATGT-3'
h*DHRS2*	5'-CCTCTGGTAGGGAGCACTCT-3'	5'-CCAGCGCCACTACTGGATTA-3'
h*PGAM2*	5'-CACCGCCTCGTGATGGTT-3'	5'-CAGCACCGACGTGTAGCAGA-3'
h*TOP2A*	5'-GTGGCAAGGATTCTGCTAGTCC-3'	5'-ACCATTCAGGCTCAACACGCTG-3'
h*E2F2*	5'-CGTCCCTGAGTTCCCAACC-3'	5'-GCGAAGTGTCATACCGAGTCTT-3'
h*C5*	5'-AGTGTGTGGAAGGGTGGAAG-3'	5'-GTTCTCTCGGGCTTCAACAG-3'
h*C3*	5'-GCCAAGACGAAGAGAA-3'	5'-GGCACCCAAAGACAAC-3'
h*C1R*	5'-TTCCCCAAGCCTTACCCCAA-3'	5'-GCTGGAAGACGAGCTTCACC-3'
h*C1S*	5'-AAGAGCGTTTTACGGGGTTT-3'	5'-AATCTCCCCAATCAGTGCAG-3'
h*F2RL2*	5'-GCAAAGCCAACCTTACCCATT-3'	5'-GAGGTAGATGGCAGGTATCAGT-3'
h*SERPINA1*	5'-TGAGGCACGATGGCAACAT-3'	5'-GAGCCCTCTCTTGATCTGGG-3'
h*CD59*	5'-CAGTGCTACAACTGTCCTAACC-3'	5'-TGAGACACGCATCAAAATCAGAT-3'
h*SERPINE1*	5'-ATTTGACGACGAATCGGACCC-3'	5'-GTTCTTGCGGTCTTTCTGGGA-3'